nature water

Article

https://doi.org/10.1038/s44221-022-00001-4

Revisiting Mt Fuji's groundwater origins with helium, vanadium and environmental DNA tracers

Received: 8 April 2022

Accepted: 10 October 2022

Published online: 19 January 2023

Check for updates

O. S. Schilling[1,2,3] ✉, K. Nagaosa[4], T. U. Schilling[5], M. S. Brennwald[2], R. Sohrin[4], Y. Tomonaga[1,2,6], P. Brunner[3], R. Kipfer[2,7] & K. Kato[4]

Known locally as the water mountain, for millennia Japan's iconic Mt Fuji has provided safe drinking water to millions of people via a vast network of groundwater and freshwater springs. Groundwater, which is recharged at high elevations, flows down Fuji's flanks within three basaltic aquifers, ultimately forming countless pristine freshwater springs among Fuji's foothills. Here we challenge the current conceptual model of Fuji being a simple system of laminar groundwater flow with little to no vertical exchange between its three aquifers. This model contrasts strongly with Fuji's extreme tectonic instability due to its unique location on top of the only known continental trench–trench–trench triple junction, its complex geology and its unusual microbial spring water communities. On the basis of a unique combination of microbial environmental DNA, vanadium and helium tracers, we provide evidence for prevailing deep circulation and a previously unknown deep groundwater contribution to Fuji's freshwater springs. The most substantial deep groundwater upwelling has been found along Japan's most tectonically active region, the Fujikawa-kako Fault Zone. Our findings broaden the hydrogeological understanding of Fuji and demonstrate the vast potential of combining environmental DNA, on-site noble gas and trace element analyses for groundwater science.

With its near-perfect conical shape, Japan's volcanic Mt Fuji (3,776 m above sea level (ASL)) may arguably be the world's best-known mountain[1]. Known locally as the water mountain, for millennia Fuji has provided safe drinking water to millions of people via its abundant groundwater and groundwater-fed springs. The abundance of freshwater resources arises from large amounts of precipitation that occur due to Fuji's proximity to the Pacific Ocean and Sea of Japan, and its unique location on top of Fuji triple junction, the only known continental trench–trench–trench triple junction on Earth[2–4] (Fig. 1). Due to this unique geologic setting, Fuji consists primarily of basalt and is much more permeable than other arc stratovolcanoes, which are mostly composed of poorly permeable andesitic magmas[5–13]. Owing to its long passage through basalt[14], Fuji's groundwater is very soft and strongly enriched in vanadium, making Fuji's rivers the most vanadium enriched on Earth[15–17]. Fuji is so important that it has UNESCO World Heritage Site status[18], with multiple springs designated as national Natural Monuments[19–21].

[1]Hydrogeology, Department of Environmental Sciences, University of Basel, Basel, Switzerland. [2]Department Water Resources and Drinking Water, Eawag–Swiss Federal Institute of Aquatic Science and Technology, Dübendorf, Switzerland. [3]Centre for Hydrogeology and Geothermics, Université de Neuchâtel, Neuchâtel, Switzerland. [4]Department of Geosciences, Shizuoka University, Shizuoka, Japan. [5]Department of Geology and Geological Engineering, Université Laval, Quebec, Quebec, Canada. [6]Entracers GmbH, Dübendorf, Switzerland. [7]Institute of Biogeochemistry and Pollutant Dynamics and Institute of Geochemistry and Petrology, Swiss Federal Institute of Technology Zurich (ETHZ), Zurich, Switzerland. ✉e-mail: oliver.schilling@unibas.ch

https://doi.org/10.1038/s44221-022-00001-4

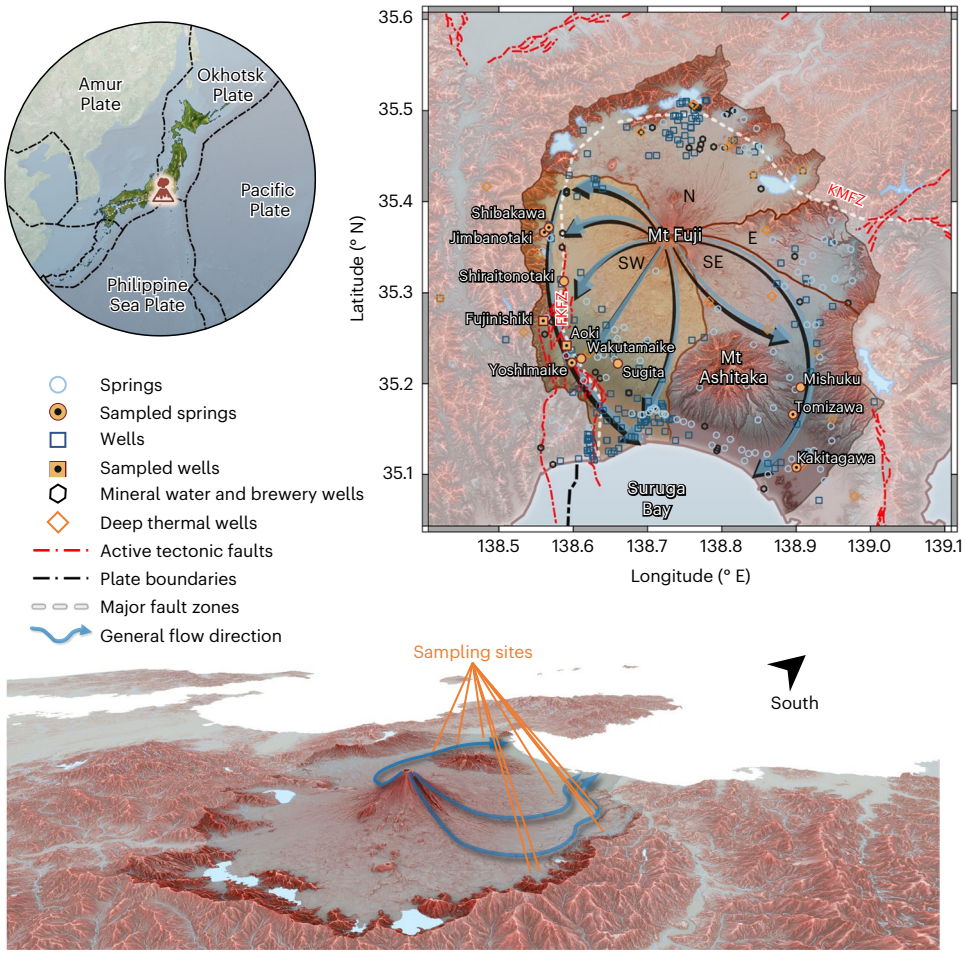

Fig. 1 | Fuji catchment. Top left: Fuji's location on the trench–trench–trench triple junction between the Amur, Okhotsk, and Philippine Sea plates in central Japan. Top right: map of Fuji catchment, its four sub-basins (with the southwestern sub-basin highlighted in yellow), the general groundwater flow directions of the southwestern and southeastern sub-basins, the major fault zones, the currently active tectonic faults, the sampled sites and all data points obtained in this study or gathered from literature and the national groundwater database of Japan. Black dots in the symbols for sampled sites indicate the locations of eDNA analyses. Bottom: 3D map of Mt Fuji oriented towards the southeast. Fuji catchment is highlighted, and the sampling sites and general flow directions of the southwestern and southeastern sub-basins are indicated. KMFZ = Kotsu-Matsuda Fault Zone. Coordinate reference system: WGS 84/ Pseudo-Mercator. Composite map sources: satellite imagery[161]; digital elevation model[162]; red 3D hillshade map[163,164]; active tectonic fault locations[165]; plate boundaries and major tectonic faults[43,166,167].

On top of the ever-increasing demand for water by residents, tourists, industry and agriculture, a microcosm of premium food industries has developed, producing goods that depend heavily on Fuji's clean water. Japan's largest green tea plantation area on the southern slopes and large whisky distilleries on the eastern slope can only operate because of the consistently large supply of soft, high-quality groundwater. With increasing success, numerous water bottling companies now sell vanadium-rich groundwater pumped from deep below Fuji as healthy mineral water[22–24]. Moreover, it was found that if vanadium-rich water is used in sake (*nihonshu*) brewing, undesired stale aroma compounds are suppressed while the desired sweet taste is fostered[25,26], potentially explaining the award-winning international success of Fuji's sake breweries[27,28].

Although Fuji has been studied extensively and its complex geology is well documented, water quality and quantity are declining and many hydrogeological questions remain unsolved[29–35]. According to current understanding, of the 2.2 km^3 (or 2,500 mm) of precipitation per year, 90% form groundwater recharge[7,36]. After 15–40 yr (ref. 14), 1.7 km^3 emerge each year at the foothills as springs, rivers and lakes, while the rest leaves the catchment as groundwater[7]. Although groundwater also flows through the deep Ko ('old')-Fuji aquifer, formed during the older Hoshiyama volcanic stage (100–17 kyr ago (ka)), springs are believed to be fed exclusively from the shallower Shin ('new')-Fuji and Surficial aquifers, originating from the younger Fujinomiya and Subashiri stages (<17 ka)[7,13,17,37,38]. Except for some seepage[31], vertical exchange between the deep and shallow aquifers is currently considered to be negligible[7,17,36,39]. This simple model, however, is at odds with Fuji's complex geology and fails to explain the decline in water quality[29,30,40–42].

Here we present evidence for a substantial contribution of Ko-Fuji deep groundwater to the springs along Fuji's Fujikawa-kako Fault Zone (FKFZ), Japan's most tectonically active region (Fig. 1)[10,43–45]. Our environmental DNA (eDNA), helium (He) and vanadium (V) measurements, together with a compilation of hydrochemical data from many earlier studies, broaden our hydrogeological understanding of Fuji and demonstrate the vast potential of combining eDNA, on-site noble gas and trace element analyses for groundwater science.

Shared meteoric origin and the limits of classic tracers

Despite its critical inability to fully explain the recent water quality decline, the simplistic conceptual model of laminar groundwater flow within Fuji is still accepted. The culprits are the classic methods that have been applied to understand Fuji's hydrogeology so far, namely

https://doi.org/10.1038/s44221-022-00001-4

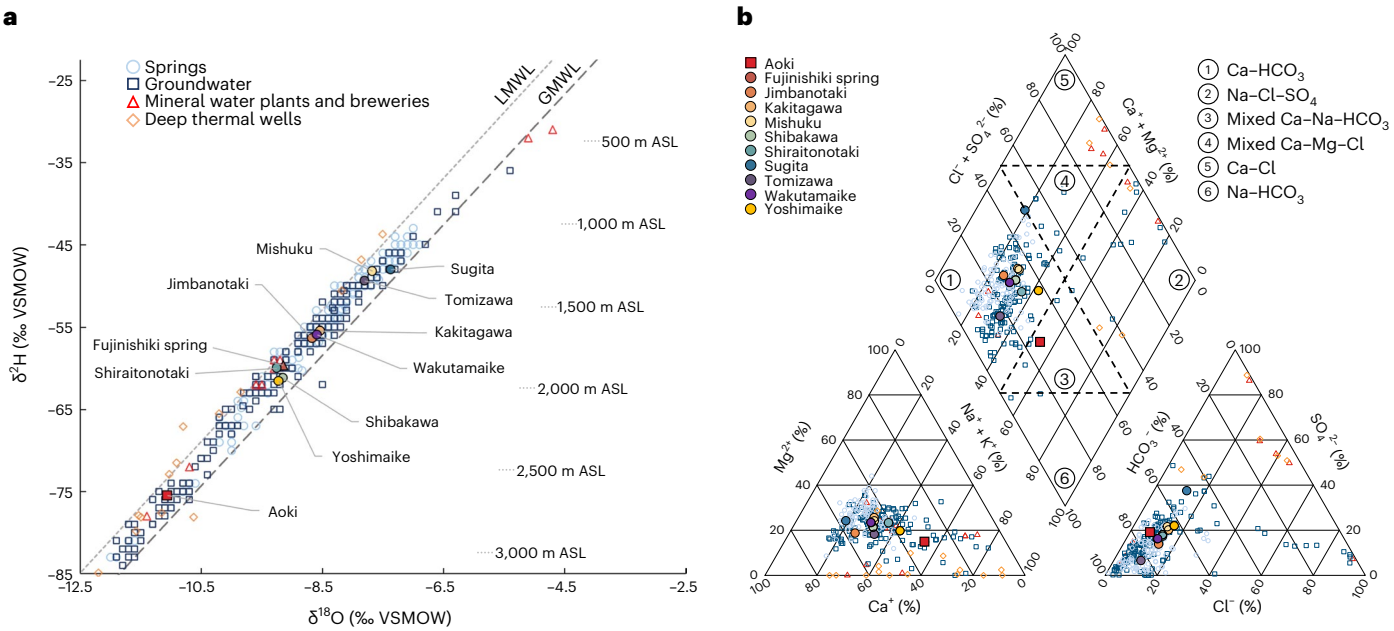

Fig. 2 | Overview of the stable water isotope and major ion compositions of springs and groundwater in Fuji catchment. a, Stable water isotope composition of investigated sites alongside all available measurements of springs, groundwater wells, mineral water and brewery wells and thermal deep wells; stable water isotope-derived recharge elevations after Yasuhara et al.[36] are indicated. Local meteoric water line (LMWL)[36]: $\delta^2H = 8 \times \delta^{18}O + 15.1‰$. Global meteoric water line (GMWL)[51]: $\delta^2H = 7.93 \times \delta^{18}O + 8.99‰$. VSMOW, Vienna standard mean ocean water. **b**, Piper plot of the major ion composition of all available data on springs, groundwater wells, mineral water and brewery wells, and thermal deep wells. The fields of hydrochemical water types are separated by dashed lines and marked by numbered circles (see legend). Data points in **a** and **b** represent site-averaged values. All individual data points and corresponding references are provided in tabular form in Supplementary Data 1.

shallow groundwater levels, major ions and stable water isotopes. These classic hydrogeological methods are the most widely employed and are typically used to identify groundwater flow directions, recharge zones and seasonality, and flow through distinct hydrochemical zones. However, in mountainous systems where shallow groundwater levels follow the topography, where physical mixing between different water types is prevalent and the major ion compositions of different water types are very similar, these classic methods often do not allow an unambiguous assessment of groundwater recharge and flow paths[36,46,47].

As the hydrogeology of Fuji is dominated by elevational gradients, shallow groundwater levels follow the general topography and provide no indication of vertical interactions between different aquifers[17,39,48,49]. The Ko-Fuji deep aquifer is known to be confined and artesian, but the pressure distribution is unknown[17,29–31,39]. Stable water isotope signatures (i.e., δ^2H & $\delta^{18}O$) of streams, springs and groundwater fall between the local and the global meteoric water lines (Fig. 2a and Supplementary Section 1), revealing a common meteoric origin and uniform evaporation effect[36,50], but recharge elevation, seasonality and physical mixing cannot be separated on the basis of those signals[51].

Springs and groundwaters around Fuji are all cold (~14.5 °C), fresh (~400 µS cm^{-1}), mildly alkaline (~7.75 pH) and classified as Ca–HCO_3 type. Along Suruga Bay, the Na–Cl–SO_4 type prevails due to local seawater intrusion[17,32,41,42] (Fig. 2b). Only deep thermal groundwaters, which are pumped from Fuji's basement from a depth of 1,500 m and used in local spas (*onsen*), are mildly warm (~40 °C), slightly alkaline (~8.75 pH) and mineralized (~1 g l^{-1}). Due to the great depth and admixture of seawater inclusions from the green tuff of Fuji's basement, this thermal water is classified as Ca–Cl and Na–Cl–SO_4[52,53]. However, besides the seawater inclusions in Fuji's basement and seawater intrusion along Suruga Bay, all natural waters in Fuji catchment are of meteoric origin[52,53]. The shared meteoric origin, large elevational range and hydrochemical similarity of the natural waters mean that the classic tracer methods employed are of limited applicability for differentiating water bodies/components. Rather than provoking further research, these observations were widely accepted and interpreted in a straightforward manner as being the result of a laminar flow system. However, this interpretation obscures potentially existing vertical interactions between the different aquifers, and instead fosters the idea of Fuji being a relatively simple groundwater system.

Deep groundwater upwelling revealed by He, V and eDNA

To overcome the limitations of the classic methods applied in Fuji catchment so far, and to critically assess the governing conceptual hydrogeological model of Fuji, we carried out a multi-tracer investigation combining three unconventional and new tracer methods: on-site and laboratory-based He, V and eDNA analyses. Below we report the major findings for each tracer, focusing on the identification of physical mixing based on concentrations of dissolved He and V, and the fraction of eDNA contributed by Archaea specifically adapted to deep groundwater conditions. Analytical data are summarized in Table 1 (the full dataset is provided as Supplementary Data 1 and 2).

Helium

Near volcanoes and plate borders, total He concentrations and the isotope ratios of $^{20}Ne/^4He$ and $^3He/^4He$ are important tracers, as they allow the contributions of atmospheric versus terrigenic He to be quantified, as well as the separation between mantle and radiogenic He[54–64]. For example, if in a volcanic and tectonically active system like Fuji catchment deep groundwater was to be found enriched in mantle He, this He signature can be used to detect the contributions of deep groundwater to shallow groundwater and constrain the origin of water at the sampled freshwater springs.

By taking the characteristic $^3He/^4He$ and $^{20}Ne/^4He$ ratios of air-saturated water ($^3He/^4He = 1.36 \times 10^{-6}$, $^{20}Ne/^4He = 3.741$)[65], depleted mantle (as sampled by mid-ocean-ridge basalt; $^3He/^4He = 1.1 \times 10^{-5}$, $^{20}Ne/^4He \approx 0$)[55] and continental crust ($^3He/^4He = 1.5 \times 10^{-8}$, $^{20}Ne/^4He \approx 0$)[57] into account, the contribution of mantle He can be calculated: 20%

https://doi.org/10.1038/s44221-022-00001-4

Table 1 | Overview of dissolved He, V and archaeal eDNA signatures of sampled springs and groundwater

Sample	ID	He ($\times10^{-8}$ cm^3_{STP} g H_2O^{-1})	$^3He/^4He$ ($\times10^{-6}$)	$^{20}Ne/^4He$	He source			V ($\mu g\,l^{-1}$)	$f_{A,YLA114}$ (%)	$f_{A,WCHD3\text{-}30}$ (%)	H'_A
					Atm	Mnt	Rad				
Southwestern sub-basin											
Aoki	A	7.1	3.01	2.829	75%	20%	5%	221.0	49.4	45.8	1.27
Shibakawa no. 1	1a	3.7	1.71[53]	3.704[53]	100%			29.0	1.0[35]	19.9[35]	1.56[35]
Shibakawa no. 2	1b	4.6[53]	1.47[96]	3.765*	100%						
Jimbanotaki	2	3.8						16.3	12.4	40.9	1.79
Shiraitonotaki no. 1	5a	3.8[53]	1.86[53]	3.333[53]	90%	5%	5%	38.8			
Shiraitonotaki no. 2	5b	5.1[96]	1.79[96]	4.208*	100%						
Sugita	16	4.2						13.9			
Fujinishiki	F1							59.4	27.5	49.5	1.56
Yoshimaike	9	7.4	3.46	2.773	75%	20%	5%	87.5	35.0	45.3	1.41
Wakutamaike	10	149[96]	1.31[96]	0.139*	5%	12.5%	82.5%	46.5			
Southeastern sub-basin											
Mishuku	63	4.6						21.9			
Tomizawa	60	4.8	1.79	3.704	100%			30.4	22.0	55.0	1.39
Kakitagawa no. 1	48a	5.2	1.54	3.668	100%			37.5	23.3	13.9	1.64
Kakitagawa no. 2	48b	4.6[102]	1.68[102]	3.930[102]	100%						

Vanadium and archaeal eDNA signatures represent site-averaged values (full dataset provided as Supplementary Data 1). The three potential He sources that can mix to produce the observed ^3He and ^4He concentrations are the atmosphere (Atm), mantle (Mnt) or radiogenic decay (Rad)[54–57]. Note that in the context of groundwater hydrology, Neon isotopes are only of atmospheric origin[55]. STP stands for standard temperature and pressure (T=0 °C, P=1 atm). $f_{A,YLA114}$ and $f_{A,WCHD3\text{-}30}$ are the fractions of archaeal eDNA contributed by the candidate extremophile Parvarchaea orders YLA114 and WCHD3-30, respectively. H'_A is Shannon's diversity index (H')[160] evaluated for Archaea. * $^{20}Ne/^{22}Ne$ ratios for these samples were not provided by Asai and Koshimizu[96] and the ratio of air-saturated water was used instead. He concentrations from this study correspond to concentrations measured on site with the new GE-MIMS instrument. Data from refs. 35, 53, 96, 102.

in the Ko-Fuji deep groundwater of Aoki well and Yoshimaike spring, 12% in Wakutamaike spring, and 5% in Shiraitonotaki (sample no. 1) (Table 1 and Fig. 3e,f). The high mantle He contributions in Aoki and Yoshimaike correlate with high total He concentrations (Table 1 and Fig. 3d,e). Hence, noble gas data suggest that Ko-Fuji deep groundwater is contributing significantly to Fuji's southwestern springs—less so at the northern, upstream end of the alluvial fans (Shibakawa, Jimbanotaki, Shiraitonotaki), but strongly in springs located directly on the FKFZ (Yoshimaike, Wakutamaike) (Figs. 1 and 3). Although the presence of mantle He in the different springs could be a result of the upwelling of Ko-Fuji deep groundwater, it could also be the result of a direct admixture of mantle gases. Additional tracers are therefore required to confirm the upwelling of Ko-Fuji deep groundwater.

The Wakutamaike spring exhibited not only a 12% contribution of mantle He, but also an 83% contribution of radiogenic He (Fig. 3e,f)—an observation that suggests a hydraulic connection to a completely different groundwater reservoir. Total He concentrations are also three orders of magnitudes larger than in any other sampled spring. The He signature is very similar to the signature of the deep thermal water pumped close to Lake Tanuki at the base of the Misaka-Tenshu Mountain range (Fig. 3e,f and Supplementary Section 3), suggesting that the complex network of faults, fissures and clinkers of the FKFZ transports groundwater from deep below the Misaka-Tenshu mountains to Wakutamaike spring with little mixing.

Vanadium

Dissolved V has been measured in Fuji's springs, groundwaters and rivers since the 1960s and is found to be enriched and prevail in oxidized form as vanadate (V(v)). Owing to the naturally high V content of basalt[66], the V concentration in Fuji's groundwater and springs is much larger than anywhere else in Japan[16,17,67–69], making Fuji's rivers the most V-enriched on Earth[15]. While V reaction kinetics in natural waters are difficult to quantify due to vanadium's highly complex geochemistry[70–74], on the scale of the decadal residence times of Fuji groundwater, equilibria concentrations are probably not reached[72,75] and V concentrations can be assumed to increase gradually with groundwater residence time. This assumption is supported by the observation that V concentrations have not reached a plateau (Fig. 3c). Thus, if a spring was to be found to be significantly enriched in V compared to the local shallow groundwaters, upwelling of deep groundwater with its significantly longer residence times is the most likely cause of enrichment.

Vanadium concentrations exhibit similar patterns to stable water isotopes and major ions, with $\delta^{18}O$ and V concentrations correlating almost perfectly and lighter waters, which are recharged at higher elevations, showing larger V concentrations (Table 1, Fig. 3a–c and Supplementary Section 2). Springs overall contain less V and are isotopically heavier than groundwater (Fig. 3a–c), confirming that most springs are fed by shallow groundwater from the Surficial and Shin-Fuji aquifers, which are generally characterized by low recharge elevations and short residence times[14,17,37]. Vanadium concentrations also positively correlate with He concentrations; that is, the He-rich waters tend to be enriched in V. With a concentration of 221.0 $\mu g\,l^{-1}$, the Ko-Fuji deep groundwater sampled in Aoki well is the most V-enriched water found around Fuji, supporting the assumption of the very long residence time of Ko-Fuji groundwater in the southwestern foot of Fuji. Remarkably, with a concentration of 87.5 $\mu g\,l^{-1}$, Yoshimaike spring contains significantly more V than all other springs in the southwestern sub-basin. Although the correlation between elevated V and elevated He concentrations in springs makes a strong case for substantial Ko-Fuji deep groundwater upwelling, elevated V concentrations in springs may also arise from increased residence times due to longer flow paths or zones of reduced hydraulic conductivity within the shallow aquifers themselves. Hence, another independent tracer is required to fully confirm the existence of substantial upwelling of deep groundwater.

Microbial eDNA

Pioneering the investigation of microbial eDNA in waters around Fuji, Segawa et al.[34] identified a potential relationship between the presence of thermophilic prokaryotes and deep groundwater flow paths through Ko-Fuji aquifer in Fuji's southwestern sub-basin. Later, Sugiyama et al.[35]

https://doi.org/10.1038/s44221-022-00001-4

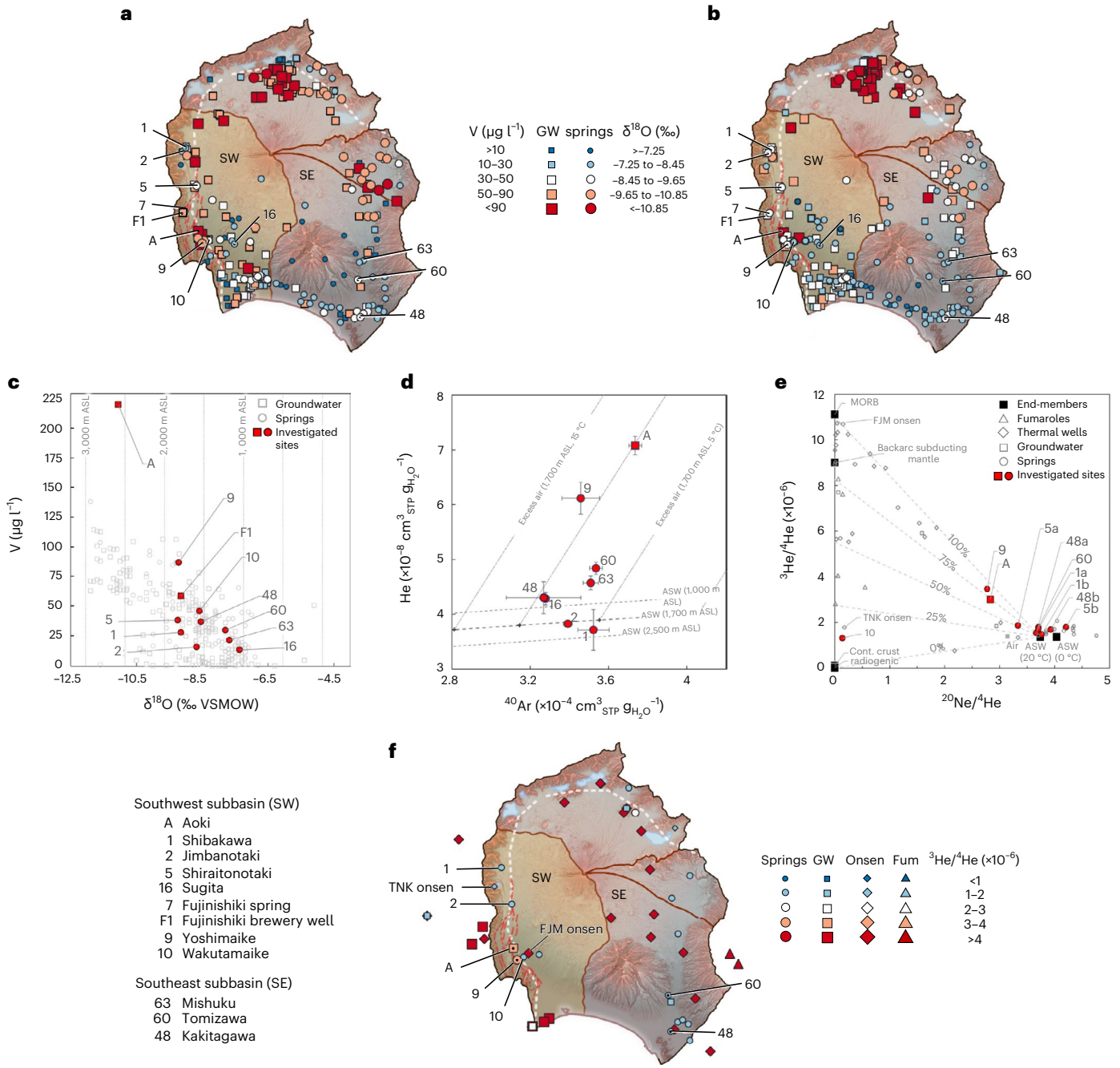

Fig. 3 | Overview of V, $\delta^{18}O$ and He compositions in springs and groundwater of Fuji catchment. a,**b**, Maps of V (**a**) and $\delta^{18}O$ (**b**) compositions. **c**, $\delta^{18}O$ versus V concentrations. Hypothetical recharge elevations (from $\delta^{18}O$ after Yasuhara et al.[36]) are indicated by dotted vertical lines assuming no mixing of waters from different elevations. **d**, Average He and ^{40}Ar concentrations measured on site with the new portable GE-MIMS instrument[133]. The black dashed lines represent air-saturated water (ASW) for 20 °C at the three primary recharge elevations after Yasuhara et al.[36] for the southwestern basin. The dotted lines indicate hypothetical excess air additions to ASW at 1,700 m ASL and for 0 °C, 5 °C, 10 °C and 15 °C. Error bars indicate ±1 s.d. of the mean of all GE-MIMS measurements taken at each site. The numbers of sampling dates used to quantify average values and standard deviations per site are: A ($n = 2$), 1 ($n = 1$), 2 ($n = 1$), 9 ($n = 2$), 16 ($n = 1$), 48 ($n = 2$), 60 ($n = 2$), 63 ($n = 1$). GW, groundwater. **e**, $^{3}He/^{4}He$ versus $^{20}Ne/^{4}He$ for samples obtained in this study (sites A, 6, 9 and 10a) alongside previous measurements (sites 1a[96], 1b[53], 3a[96], 3b[53], 7[96] and 10b[102] and data from onsen deep wells[53,104,107,111], groundwater wells[53] and fumaroles[57]) and end-member isotopic ratios[55,57] (mid-ocean ridge basalt (MORB), continental crust, radiogenic production, ASW at 0 °C and ASW at 20 °C). **f**, Overview map of $^{3}He/^{4}He$ ratios. TNK, Lake Tanuki. FJM, Fujinomiya. Fum, Fumaroles. For all data and corresponding references, see Supplementary Data 1. Coordinate reference system: WGS 84 / Pseudo-Mercator. Background composite map sources: digital elevation model[162]; red 3D hillshade map[163,164]; active tectonic fault locations[165]; plate boundaries and major tectonic faults[43,166,167]. White dashed lines in **a**, **b** and **f** indicate the FKFZ and KMFZ tectonic zones; red dashed lines in **a**, **b** and **f** indicate active tectonic faults.

confirmed that candidate extremophilic prokaryotes are cornerstone organisms in Ko-Fuji aquifer, and observed that a typhoon-induced torrential rainfall event resulted in substantially increased concentrations of suspended Archaea in Aoki well. Revisiting the eDNA data of Sugiyama et al.[35], we found members of Parvarchaea to be the dominant Archaea in Fuji groundwaters; specifically, the two uncultivated candidate orders YLA114 and WCHD3-30, which are primarily retrieved from extreme environments[76,77] (Table 1; a detailed phylogeny is provided in

https://doi.org/10.1038/s44221-022-00001-4

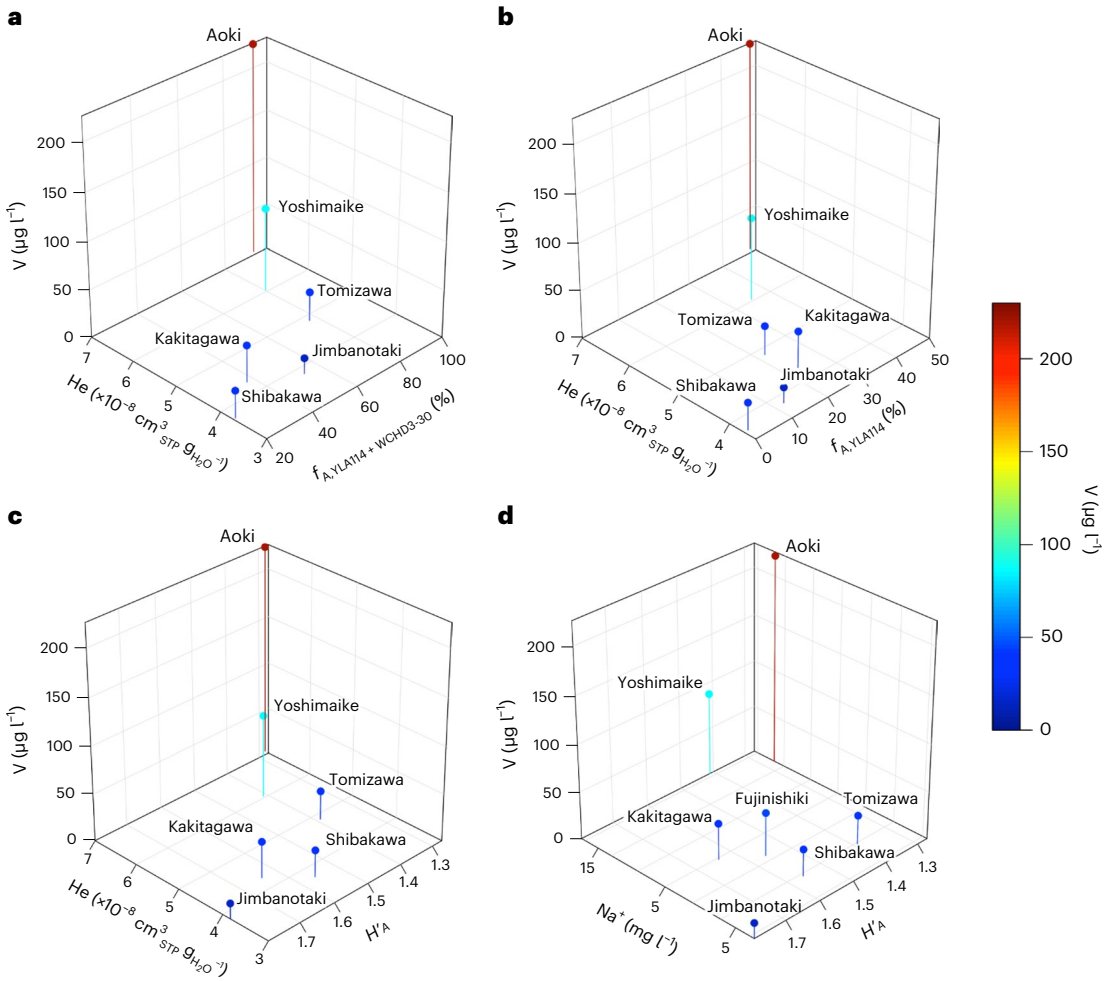

Fig. 4 | Triple tracer correlations between V, He and eDNA in Fuji catchment. **a**–**b**, Triple tracer correlations between V, He and archaeal eDNA contributed by YLA114 + WCHD3-30 (**a**) and by YLA114 only (**b**). **c,** Triple tracer correlation between V, He and the alpha diversity of Archaea. **d**, Triple tracer correlation between V, Na^+ and the alpha diversity of Archaea (**d**). He concentrations represent measurements taken on site with the new portable GE-MIMS instrument. STP, standard temperature and pressure ($T = 0$ °C, $P = 1$ atm). H'_A is Shannon's diversity index[160,168] evaluated for Archaea. Data for Fujinishiki in **d** represent data from Fujinishiki brewery well (site id: F1), except for the Na^+ concentration, which represents the average measured Na^+ concentration in Fujinishiki spring (site id: 7) located next to the Fujinishiki brewery well.

Supplementary Section 4). Although the total number of Archaea in suspension increased during the typhoon-induced torrential rainfall event, the relative contributions of WCHD3-30 and YLA114 decreased, indicating that WCHD3-30 and YLA114 are primarily living in suspension rather than attached to the aquifer matrix, and that their relative contributions are reduced when increased hydraulic gradients lead to an increased detachment of Archaea that live attached on the matrix under normal hydraulic conditions. This property makes both WCHD3-30 and YLA114 potential tracers of upwelling of deep groundwater into shallow groundwater and springs in Fuji catchment even under normal hydraulic conditions. As the environmental conditions that allow these specific Archaea to develop have so far been found around Fuji only at great depths[17,52,78,79], the presence of the DNA of these microbial life forms in springs is furthermore likely to be indicative of fast upwelling of a significant amount of deep Ko-Fuji groundwater, as these specific DNA would otherwise not exist or be degraded (in the case of marginal or slow deep groundwater upwelling).

To confirm the previously identified link between the presence of these specific prokaryotes and the environmental conditions prevalent in Ko-Fuji deep groundwater[34,35], and to allow comparison between dissolved He, V and eDNA, we also determined the microbial eDNA present in water samples of the investigated springs and Aoki well. This revealed that Parvarchaea account for 95% of all archaeal eDNA present in the Ko-Fuji groundwater of Aoki well (Table 1 and Supplementary Section 4). While in the most upstream of the sampled southwestern springs (Shibakawa), Parvarchaea account for only 20% of archaeal eDNA, this percentage increases gradually in the downstream direction and reaches 80% in Yoshimaike spring. Parvarchaea are also the most important Archaea in Tomizawa (77%), an upstream southeastern spring emerging at the foot of Mt Ashitaka, and also present in significant levels (albeit not as dominant) in Kakitagawa (37%), the largest and most downstream spring of the southeastern sub-basin (Fig. 1). The clear spatial distribution of these Parvarchaea (that is, their comparably high abundance in downstream springs in the southwestern and southeastern sub-basins) thus makes a strong case for spatially increasing upwelling of Ko-Fuji deep groundwater in the downstream direction, particularly along the FKFZ. However, despite archaeal eDNA patterns agreeing with patterns in He and V concentrations, only a systematic comparison between these three different and completely independent tracers would allow the possibility of those Parvarchaea growing locally in springs in significant levels to be excluded and provide proof that Ko-Fuji deep groundwater is indeed upwelling.

https://doi.org/10.1038/s44221-022-00001-4

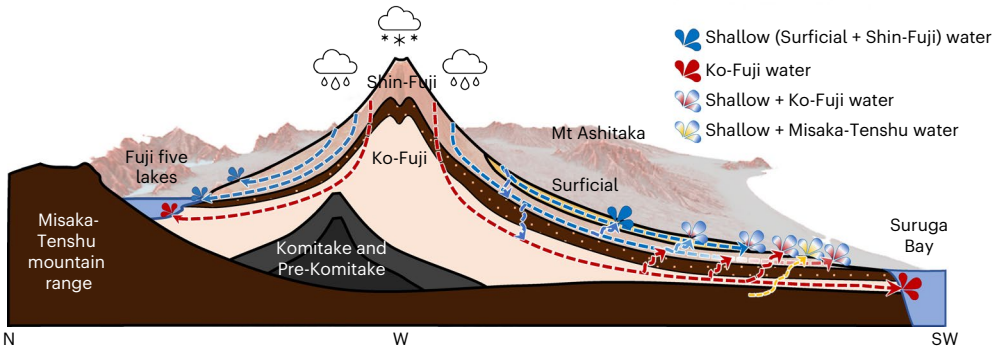

Fig. 5 | Revised conceptual hydrogeological model of Mt Fuji. The revised conceptual hydrogeological model of Mt Fuji (revised based on previously published conceptual models[7,17,36,42,169]) shows a north–southwest cross-section that follows the FKFZ and illustrates the prevailing vertical interactions between the three different principal aquifers (Surficial, Shin-Fuji and Ko-Fuji) and the resulting spring water origins. The contribution of Misaka-Tenshu deep groundwater to the sacred Wakutamaike spring is also illustrated. Blue arrows indicate shallow groundwater, red arrows Ko-Fuji groundwater and yellow arrows Misaka-Tenshu groundwater flow. Background composite map sources: digital elevation model[162]; red 3D hillshade map[163,164].

Table 2 | Overview of investigated springs and artesian groundwater wells

Site	Id	Latitude (° N)	Longitude (° E)	Elevation (m ASL)	Well depth (m)	Type	Major ions	δ^2H & $\delta^{18}O$	Residence time	$^{87}Sr/^{86}Sr$	V	NG	TDC	eDNA
Shibakawa	1	35.3717	138.5672	715		spring	x,o	x,o	o	o	o	x,o	x,o	o
Jimbanotaki	2	35.3663	138.5612	695		spring	x,o	x,o	o	o	o	x	x,o	x
Shiraitonotaki	5	35.3128	138.5876	480		spring	o	o	o	o	o	o		
Fujinishiki	7	35.2692	138.5597	230		spring	o	o	o	o	o			
	F1	35.2692	138.5597	230	32	well		x			x		x	x
Yoshimaike	9	35.2231	138.5982	130		spring	x,o	x,o	o	o	x,o	x	x,o	x
Wakutamaike	10	35.2276	138.6108	120		spring	o	o	o	o	o	o	x,o	
Aoki	A	35.2420	138.5910	140	550	well	x,o	o			x	x	x,o	x
Sugita	16	35.2221	138.6600	195		spring	o	x,o	o	o	o	x	x,o	
Mishuku	63	35.1961	138.9059	175		spring	o	x,o	o		o	x	x,o	
Tomizawa	60	35.1662	138.8956	110		spring	x,o	x,o	o		o	x	x,o	x
Kakitagawa	48	35.1077	138.9003	15		spring	x,o	x,o	o	o	x,o	x,o	x,o	x

NG, noble gases; TDC, microbial total direct cell counts. Data for Fujinishiki are composed of data from the Fujinishiki sake brewery's artesian well (site id: F1; all data except for major ions and Sr isotope ratios) and Fujinishiki spring (site id: 7) located next to the well. x, this study; o, existing literature.

Evidence for mixing of groundwaters from different depths

To identify whether the three independent tracers indicate substantial upwelling of Ko-Fuji deep groundwater into the springs along the FKFZ, they are directly compared in four triple tracer plots (Fig. 4). Comparing the concentrations of dissolved V and He to the fractions of archaeal eDNA contributed by YLA114 (Fig. 4a) and by YLA114 + WCHD3-30 (Fig. 4b) reveals that the three tracers are nearly linearly correlated. The near-linear correlation prevails if concentrations of V and He are compared with the alpha diversity of Archaea (Fig. 4c). As all three tracer types have completely different biogeochemical origins, the only plausible explanation for the near-linear correlation, given current knowledge of the system, is physical mixing processes (upwelling and increasing admixture in the downstream direction) of Ko-Fuji deep groundwater into the shallow aquifers and freshwater springs of Fuji.

The identified triple tracer correlation between He, V and extremophile archaeal eDNA, in combination with the near-linear correlations between V and $\delta^{18}O$, He concentrations and $^3He/^4He$ ratios and the relative abundance of the YLA114 and WCHD3-30 Archaea orders, provide strikingly strong evidence for widespread upwelling and admixture of Ko-Fuji deep groundwater into the springs and shallow aquifers of Fuji.

The rate of upwelling of deep groundwater is far greater than previously assumed, particularly in the most densely populated southwestern sub-basin. The currently accepted hydrogeological model, which postulates negligible to no vertical mixing between the different groundwater bodies, is incompatible with the new tracer data and therefore needs to be revised. We propose a revised conceptual hydrological flow model of Fuji that explicitly assumes substantial upwelling of Ko-Fuji deep groundwater along the faults, fissures and clinkers of the FKFZ, which are a result of the complex subduction dynamics of Fuji triple junction (Fig. 5). In addition to these interaction pathways, we identified a previously unknown admixture of heavy He-enriched Misaka-Tenshu-type deep groundwater in Wakutamaike spring. Wakutamaike spring, coincidentially, is the sacred spring of Fujisan Hongu Sengen Taisha shrine, UNESCO World Heritage Site and one of Japan's most important shrines.

Conclusions

While groundwater level observations and classic hydrological tracers such as major ions and stable water isotope compositions of groundwater and spring water can provide valuable insights into hydrogeological systems, they cannot detect the vertical exchange between the different aquifers of Mt Fuji. Although applied widely, they are of limited use in

many complex environments, as classic tracers are often confounded by interactions with the aquifer matrix, which typically consists of largely the same material and thus harmonizes the chemical composition of different waters, or by recharge zones that overlap, which harmonize the isotope compositions of different waters. By combining multiple classic and unconventional tracers—namely on-site analysis of dissolved (noble) gases, laboratory-based analysis of noble gas isotopes, next-generation sequencing of microbial eDNA, and the analysis of trace elements, all of which are tracers that specifically react to the variety in flow paths and processes that can be expected in a volcanic system such as Fuji catchment, and allow us to disentangle and therefore track waters that are subject to physical mixing—we not only overcame the principal limitations of the classic methods, but also demonstrated a clear way forward for groundwater science.

In conclusion, advances in analytical techniques in tracer hydrology and microbiology enabled us to understand the complex hydrogeology of the volcanic groundwater system of Fuji and to identify previously unknown upwelling of deep groundwater into freshwater springs and shallow groundwater. The combination of He, V and microbial eDNA signatures thus not only broadens the hydrogeological understanding of Fuji, but also showcases the vast potential of combining unconventional tracers to study complex hydrogeological systems.

Methods

Study site and current challenges

As a result of its location directly on top of the triple junction between the Okhotsk, Amur and Philippine Sea plates, Mt Fuji's ejecta consist primarily of high-alumina basalt and volcanic ash, as opposed to the andesitic composition that most other stratovolcanoes located on the Izu–Bonin–Mariana arc eject[6]. The basaltic composition provides evidence that Fuji's magma reservoir is located at a great depth (>20 km)[6,11,12,80–84]. Fuji consists of four volcanoes that grew on top of each other: Pre-Komitake (270–160 ka), Komitake (160–100 ka), Ko-Fuji (100–10 ka) and Shin-Fuji (10 ka to present)[1,6,38,81,85,86]. The deposits of the late Hoshiyama volcanic stage (100–17 ka) and deposits of the Fujinomiya and Subashiri stages (<17 ka)[9,13,17,31,35,37,39,87–89] are of hydrogeological relevance. Late Hoshiyama deposits consist of basaltic lava, volcanic ash and respective mudflows, and host the deep Ko-Fuji aquifer. Ko-Fuji aquifer is confined on top by largely impermeable mudflow deposits (hydraulic conductivities between 10^{-6} m s^{-1} (horizontal) and 10^{-8} m s^{-1} (vertical); ref. 42), pyroclastic rocks and Fuji black soil of the final Hoshiyama and initial Fujinomiya stages[6,9,17,37,38,81,85,90]. The estimated hydraulic conductivity of Ko-Fuji aquifer is in the range of 10^{-5}–10^{-7} m s^{-1} (refs. 9, 39, 42, 91). The Funjinomiya and Subashiri stage deposits host the shallow Shin-Fuji aquifer, which consist of multiple basaltic lava layers that form a complex and highly conductive network of porous material, fissures and clinkers[7,17,31,37]. The most recent volcanic ash and alluvial sand and gravel deposits of the Subashiri stage finish off the hydrogeological stratigraphy by hosting the uppermost Surficial aquifer[31]. The estimated hydraulic conductivities of the Shin-Fuji and Surficial aquifers are 10^{-2}–10^{-5} m s^{-1} (refs. 9, 39, 42, 91). Underneath, the described hydrogeological system of Fuji is constrained by an approximately 10-km thick basement body of the Misaka-Tenshu group, which consists of impermeable submarine basaltic andesite and pyroclastic material[52]. The FKFZ, Japan's tectonically most active structure, is located along the west and southwest foot of Fuji and passes the city of Fujinomiya[10,43–45]. These active tectonic faults are characterized by complex fissure and clinker networks, which might allow groundwater, solutes and small particles to be transported in a non-laminar fashion and make their flow paths very difficult to identify. Hydrogeological properties of the FKFZ, as well as its effect on groundwater dynamics and flow paths, have not been systematically investigated and, while geologically relatively well understood[45], its hydrogeological behaviour remained unknown before our study.

At Fuji's summit, the mean annual air temperature is −6.4 °C, and the mean temperature during the warmest month (August) is 6.0 °C (ref. 92). Annual rainfall ranges from 1,600–2,000 mm, depending on the orientation[9,93]. Snowfall occurs throughout the year and amounts to an annual total of 3 m at the summit[92]. These winter hydrological conditions sustain a layer of permafrost near the summit, effectively preventing any infiltration into the subsurface[36,94]. However, conditions are slowly changing as a result of climate change (for example, mean maximum temperatures during the summer months have risen by 2 °C during the past 50 yr and the timberline is climbing[95]). Of the 2.2 km^3 of precipitation that fall on Fuji each year, 2 km^3 infiltrate and form groundwater that feeds Fuji's three aquifers (the Surficial, Shin-Fuji and Ko-Fuji aquifers). Groundwater then flows down Fuji's flanks and, after 2–4 decades[14,96], 1.7 km^3 emerge again each year in the foothills, feeding countless springs, rivers and lakes[37,39,49,52]. The remaining 0.3 km^3 leave the catchment as regional groundwater (for example, towards Katsura River Valley in the north) or as submarine groundwater discharge (to Suruga Bay to the south[33]).

According to stable water isotopes, groundwater recharge on Fuji occurs at three different elevations: above 2,000 m ASL (upper zone), between 1,100 and 2,000 m ASL (intermediate zone) and below 1,100 m ASL (spring zone)[9,17,36,50]. Recharge in the southwestern sub-basin occurs primarily between 1,600 and 2,250 m ASL, with the bulk of recharge taking place in the intermediate zone and feeding Shin-Fuji aquifer[36]. While the upper zone is of little importance for bulk groundwater recharge, it is the principal zone for recharge of Ko-Fuji aquifer[36]. The spring zone is characterized by (1) the emergence of a large amount of groundwater into the countless freshwater springs located along the end of the Shin-Fuji lava formation, (2) dynamic exchanges between springs, streams, rivers and shallow groundwater, and (3) agricultural, urban and industrial water use. In contrast to many regions around Japan, Fuji's natural springs are exclusively cold-water springs, and the spas that advertise as "hot springs" (*onsen*) around Fuji pump their water from Fuji's basement at a relatively uniform depth of 1,500 m.

Fuji is also known as the water mountain in Japan and is well known for its pristine and abundant springs and groundwater. Owing to its long residence time in basaltic rocks, Fuji's springs and groundwater are very soft (that is, devoid of carbonates) and naturally enriched in V, making the water important for green tea cultivation and mineral health water, whiskey and sake production[15–17,22,23,25–28,97]. Fuji's water quality and abundance, however, have been in steady decline throughout the past few decades, resulting in the region around Fuji not receiving the originally envisaged UNESCO World Natural Heritage Site designation and instead 'only' a UNESCO World Cultural Heritage Site denomination, as the environmental requirements for the former were too strict[29]. The decline in Fuji's water quality and quantity is mainly related to the steady decline in lake and groundwater levels due to over-pumping, widespread groundwater pollution due to industry and paper production, excessive nutrient inputs (for example, nitrate) from green tea cultivation, increasing water temperatures and changes in the hydrological cycle due to climate change, and illegal waste dumping[1,18,29–31,39,98]. In this context, the most impacted region is the urbanized area surrounding Fujinomiya, which is affected by industry, large green tea plantations in the uphill slopes, and the FKFZ (Fig. 1), within which the groundwater dynamics are only vaguely understood[17,34,35,99]. Because the conceptual notion of purely laminar groundwater flow persisted and led to an inability to close the local water balance of Fuji catchment, important groundwater pathways and fluxes remained unidentified[29,30]. Understanding the pathways and associated flow fields, however, is a precondition for preventing and managing contamination of groundwater and springs.

Investigated sites and existing data

While we present data for the entire Fuji catchment, our focus was on identifying the origins of the water in the freshwater springs along the

southwestern foot of Fuji, as it is that region that is most affected by both agriculture and industry, while at the same time being the most complex hydrogeologically due to the FKFZ. The investigated springs and artesian groundwater wells are hydrologically important features and are all located along the principal groundwater flow directions in the southwestern sub-basin (flow direction: Shibakawa spring, Sugita spring, Jimbanotaki spring, Shiraitonotaki spring, Fujinishiki sake brewery artesian well, Aoki artesian well, Yoshimaike spring, Wakutamaike spring; Fig. 1). Many of the sites sit directly on top of the FKFZ, where groundwater dynamics between the different aquifers, springs and surface water bodies are expected to be highly complex. For example, in response to the M_w 5.9 East Shizuoka earthquake in March 2011, which itself was triggered by the major M_w 9 Tohoku Oki earthquake, several springs and groundwater wells overflowed[30,43,44,100,101]. To complete a regional understanding of groundwater dynamics, three important springs of the southeastern sub-basin were also investigated (flow direction: Mishuku spring, Tomizawa spring, Kakitagawa spring; Fig. 1). Table 2 lists the different tracer analyses available for these sites and includes our measurements, as well as older data available from the literature.

We compiled our measurements and the available literature data into a hydrogeological dataset on Fuji catchment, encompassing more than 350 sites and over 9,500 individual data points[7,14,17,31,34,35,37,41,48,52,53,57,87,88,96,97,99,102–116]. All sites for which hydrochemical data were available that we addressed here are marked in Fig. 1. The complete dataset is provided as Supplementary Data 1, except for the microbial eDNA-based phylogenetic data, which are provided as Supplementary Data 2.

Major ions and stable water isotope analyses

For the analysis of stable water isotopes and major ions, samples were filtered with a 0.22 µm Millex-GS filter (Merck Millipore) and stored at −20 °C and 4 °C, respectively, before analysis. Major ion compositions were analysed at Shizuoka University using a Dionex ICS-3000 ion chromatograph (Thermo Fisher). Stable water isotopes were analysed by Shoko Science Co Ltd (using a Picarro L2120-*i* cavity ring-down spectrometer, Picarro, Inc.), normalized to the VSMOW and reported in δ notation[117] (typical analytical errors are ±0.2‰ for δ^2H and ±0.05‰ for $\delta^{18}O$).

V and Sr isotope analyses

Owing to their low abundance and very diverse concentrations and isotopic ratios in different rocks and minerals, V concentrations and Sr isotopes are powerful geochemical tracers of groundwater flow and proxies of groundwater residence times[118,119]. Vanadium in groundwater originates from alkaline rocks in contact with oxidized water, and is found to increase with groundwater residence times[16,70,71,120]. Vanadium dissolution is geochemically similar to Sr enrichment in groundwater. In groundwater hydrology, the $^{87}Sr/^{86}Sr$ isotopic ratio is widely employed as a tracer to track exchanges with different rocks and minerals[119,121–124]. As water–rock exchange processes depend on time, V concentrations and $^{87}Sr/^{86}Sr$ ratios tend to correlate with, and (under certain constraints) might be indicative of, groundwater residence times[46,51,125].

Vanadium water samples were filtered using a 0.22 µm Millex-GS filter (Merck Millipore) and acidified to a pH below 2 using nitric acid. The filters were washed with 10% hydrochloric acid and 0.1 M nitric acid before use. Vanadium concentrations were analysed using a polarized Zeeman Z-3700 atomic absorption spectrophotometer (Hitachi High-Tech) at Shizuoka University after dilution with 0.1 M nitric acid by 10% (typical analytical error ±4%). Strontium isotopic ratios were taken exclusively from the literature.

Dissolved (noble) gas analyses

Concentrations of dissolved noble gases and their isotopic ratios have been employed as groundwater tracers in many hydrogeological contexts, ranging from palaeotemperature reconstruction, excess air quantification, recharge elevation identification, and the quantification of the mixing of waters of different origins[55,126–132].

On-site dissolved (noble) gas analyses were carried out using gas equilibrium-membrane inlet mass spectrometry (GE-MIMS)[133]. GE-MIMS allows simultaneous measurement of inert and reactive gases (He, ^{40}Ar, ^{84}Kr, N_2, O_2, CO_2, H_2 and CH_4) in air and dissolved in water directly on-site, in near real time (complete analysis ~15 min) and with typical analytical uncertainty of ±1–3% (ref. 133). For the dissolved gas analyses, groundwater was pumped through a flow-through membrane contactor (G542 Liqui-Cel MiniModule, 3 M) at approximately 2 l min^{-1} using a peristaltic pump. The extracted gases were subsequently transferred via a 10 m stainless steel capillary to a quadrupole mass spectrometer (RGA 200, Stanford Research Systems) for final detection. For ^{40}Ar, N_2, O_2 and CO_2, which are more abundant, each data point represents the average of five individual measurements taken over a roughly 2-min period, with standard errors being approximated by the standard deviation of these five measurements. For the comparably less abundant gases ^4He, ^{84}Kr and CH_4, each data point represents the average of 15 individual measurements taken over an approximately 4-min period, with standard errors being approximated by the standard deviation of these 15 measurements. For more experimental detail, refer to refs. 133, 134. Mass spectrometric data were processed using the ruediPy package (v2019)[135] in Python (v3.8)[136].

High-resolution noble gas isotope analyses were carried out on samples of approximately 25 g of water collected in copper tubes[126] at the Swiss Federal Institute of Technology Zurich following standard protocols (see ref. 137; typical analytical errors are <1% for He and Ne concentrations, and <0.5% for isotopic ratios). As the standard protocol by Beyerle et al.[137] employs the standard atmospheric ratio of $^3He/^4He$ (R_a) of 1.384×10^{-6} as determined by Clarke et al.[138], the few literature-based dissolved $^3He/^4He$ ratios (R) reported in the R/R_a format were converted to the $^3He/^4He$ format on the basis of this ratio.

Microbial eDNA analyses

Microorganisms have been used intensively to study biogeochemical processes in surface water and groundwater, but only few studies have used microorganisms to study physical processes such as groundwater flow paths or groundwater mixing[139–142]. Recently, however, conceptual understanding of the movement of microorganisms in groundwater has improved, and it is now more widely acknowledged that microorganisms can travel over considerable distances[35,143,144] and can survive for years[145]. These aspects make microorganisms promising tracers of groundwater flow over relevant spatial and temporal scales. Furthermore, next-generation sequencing now allows the phylogenetic composition and functions of microbial communities to be identified on the basis of the analysis of microbial eDNA present in water samples in an affordable, quantitative and highly efficient manner[146].

Water samples for the analysis of microbial eDNA were collected in this study by filtering 10 l of water using 0.22 µm Sterivex-GV filters (EMD Millipore). DNA extraction was carried out at Shizuoka University using standard protocols[147], whereby prokaryotic cells were first lysed from the 0.22 µm Sterivex-GV filter units by adding a solution of lysozyme and proteinase K. Bulk DNA was then extracted using a phenol–chloroform–isoamyl alcohol mixture[148] and subsequently quantitatively determined by spectrophotometry using a NanoVue spectrophotometer (GE Healthcare UK Ltd). Amplification and sequencing were carried out by Bioengineering Lab Co. Ltd. In a two-step PCR, the hypervariable V3–V4 regions of the bacterial and archaeal 16S rRNA gene were amplified using the universal 341F/805R primer pair. In the first PCR step, the 1st-341f_MIX (5′-ACACTCTTTCCCTACACGACGCTCTTCCGATCT-NNNNN-CCTACGGGNGGCWGCAG-3′)/1st-805r_MIX (5′-GTGACTGGAGTTCAGACGTGTGCTCTTCCGATCT-NNNNN-GACTACHVGGGTATCTAATCC-3′) primer pair was used and, after purification of the PCR products, in a second PCR step the 2ndF (5′-AATGATACGGCGACCACCGAGATCTACAC-ACACTCTTTCCCTACACGACGC-3′)/2ndR

(5′-CAAGCAGAAGACGGCATACGAGAT- GTGACTGGAGTTCAGACGT-GTG-3′) primer pair was used[149–151]. Sample libraries for next-generation sequencing with MiSeq (Illumina Inc.) were prepared using the MiSeq Reagent Kit v3 (Illumina Inc.), following manufacturer protocols. Amplicon sequencing was done via paired-end sequencing (2 × 300 bp) on the MiSeq platform. Operational taxonomic units were clustered at a 97% similarity level using QIIME 2[152,153] and assigned on the basis of representative sequences by comparison against the GreenGenes database (v13.8)[154,155]. Patterns in the microbial community structure were explored using the phyloseq package (v1.30.00)[156] in R (v3.6.2)[157]. The nucleotide sequence datasets obtained in this study have been filed in the DNA Databank of Japan (DDBJ) under accession number DRA013474.

Microbial enumeration based on total direct counts

Total direct counts of microbial cells (a rapid method for the quantification of both culturable and unculturable microorganisms in environmental samples) were conducted at Shizuoka University following standard procedures[158]. A 100 ml water sample was collected on a 0.2 µm Nuclepor filter (GE Healthcare UK Ltd) and fixed with pH-neutral formaldehyde. The prokaryotic cells captured on the filter were then stained with 0.01 µg ml^{-1} fluorescent 4′,6-diamidino-2-phenylindole (Nacalai Tesque Inc.) and counted optically (using a BX51-FLA epifluorescence microscope equipped with a DP71 camera (Olympus)).

Reporting summary

Further information on research design is available in the Nature Portfolio Reporting Summary linked to this article.

Data availability

All data used in this study are compiled into Supplementary Data 1 and 2 and are available via the public data repository HydroShare at https://doi.org/10.4211/hs.4eac370d12e142b5aa718e5deb57da39 (ref.159). The nucleotide sequence datasets obtained in this study are filed in the DNA Databank of Japan (DDBJ) under accession number DRA013474. Unless stated otherwise, hydrogeochemical and map background data were obtained with the open-source web browser Mozilla Firefox (v.68-v98), maps were generated with the open-source geographical information system QGIS (v3.6-v3.18) and data were processed with Microsoft Office (v2016-v2019) for Mac.

References

1. Chakraborty, A. & Jones, T. E. in *Natural Heritage of Japan Geoheritage, Geoparks and Geotourism (Conservation and Management Series)* (eds Chakraborty, A. et al.) Ch. 16 (Springer, 2018).
2. Nakamura, K. Possible nascent trench along the eastern Japan Sea as the convergent boundary between Eurasian and North American plates (in Japanese). *Bull. Earthq. Res. Inst.* **58**, 711–722 (1983).
3. Seno, T. Is northern Honshu a microplate? *Tectonophysics* **115**, 177–196 (1985).
4. Ogawa, Y., Takami, Y. & Takazawa, S. in *Formation and Applications of the Sedimentary Record in Arc Collision Zones* Vol. 436 (eds Draut, A. E. at al.) 155–170 (Geological Society of America, 2008).
5. Tsuya, H. & Morimoto, R. Types of volcanic eruptions in Japan (in Japanese). *Bull. Volcanol.* **26**, 209–222 (1963).
6. Aoki, Y., Tsunematsu, K. & Yoshimoto, M. Recent progress of geophysical and geological studies of Mt. Fuji Volcano, Japan. *Earth Sci. Rev.* **194**, 264–282 (2019).
7. Tsuchi, R. Geology and groundwater of Mt. Fuji, Japan (in Japanese). *J. Geogr.* **126**, 33–42 (2017).
8. Vittecoq, B., Reninger, P.-A., Lacquement, F., Martelet, G. & Violette, S. Hydrogeological conceptual model of andesitic watersheds revealed by high-resolution heliborne geophysics. *Hydrol. Earth Sys. Sci.* **23**, 2321–2338 (2019).
9. Yamamoto, S. Hydrologic study of volcano Fuji and its adjacent areas (in Japanese). *Geogr. Rev. Jpn* **43**, 267–184 (1970).
10. Yamamoto, T. & Nakada, S. in *Volcanic Hazards, Risks, and Disasters* (eds Shroder, J. F. & Papale, P.) 355–376 (Elsevier, 2015).
11. Hasegawa, A. et al. Plate subduction, and generation of earthquakes and magmas in Japan as inferred from seismic observations: an overview. *Gondwana Res.* **16**, 370–400 (2009).
12. Kashiwagi, H. & Nakajima, J. Three-dimensional seismic attenuation structure of central Japan and deep sources of arc magmatism. *Geophys. Res. Lett.* **46**, 13746–13755 (2019).
13. Obrochta, S. P. et al. Mt. Fuji Holocene eruption history reconstructed from proximal lake sediments and high-density radiocarbon dating. *Quat. Sci. Rev.* **200**, 395–405 (2018).
14. Tosaki, Y. & Asai, K. Groundwater ages in Mt. Fuji (in Japanese). *J. Geogr.* **126**, 89–104 (2017).
15. Imtiaz, M. et al. Vanadium, recent advancements and research prospects: a review. *Environ. Int.* **80**, 79–88 (2015).
16. Koshimizu, S., & Tomura, K. (2000). Geochemical behavior of trace vanadium in the spring, groundwater and lake water at the foot of Mt. Fuji, Central Japan. In K. Sato & Y. Iwasa (Eds.), *Groundwater Updates*. Springer, Tokyo. 171-176. https://doi.org/10.1007/978-4-431-68442-8_29
17. Ono, M. et al. Regional groundwater flow system in a stratovolcano adjacent to a coastal area: a case study of Mt. Fuji and Suruga Bay, Japan. *Hydrogeol. J.* **27**, 717–730 (2019).
18. UNESCO *Fujisan, Sacred Place and Source of Artistic Inspiration* (World Heritage Convention, 2013); https://whc.unesco.org/en/list/1418
19. *Nationally Designated Cultural Properties Database* (in Japanese) (Agency of Cultural Affairs Japan, 2020); https://kunishitei.bunka.go.jp/bsys/index
20. *Showa's 100 Famous Waters of Japan* (Ministry of the Environment Japan (MOEJ), 1985); https://www.env.go.jp/water/meisui/
21. *Heisei's 100 Famous Waters of Japan* (MOEJ, 2009): https://www.env.go.jp/water/meisui/
22. *An Overview of the Bottled Water Market in Japan* (Frost & Sullivan, 2016).
23. Fujiyoshida Mineral Water Conservation Association *FMWCA Regulations* (in Japanese) (Mt. Fuji Springs Inc., 2016); http://fujiyoshida-hozen.org/aboutwater/
24. Adachi, Y. et al. The physiological effects of the undercurrent water from Mt. Fuji on type 2 diabetic KK-Ay mice. *Biomed. Res. Trace Elem.* **15**, 76–78 (2004).
25. Isogai, A., Kanada, R., Iawata, H. & Sudo, S. The influence of vanadium on the components of hineka (in Japanese). *J. Brew. Soc. Jpn* **107**, 443–450 (2012).
26. Tamada, Y., Tokui, M., Yamashita, N., Kubodera, T. & Akashi, T. Analyzing the relationship between the inorganic element profile of sake dilution water and dimethyl trisulfide formation using multi-element profiling. *J. Biosci. Bioeng.* **127**, 710–713 (2019).
27. *London Sake Challenge 2018: Awarded Sake* (Sake Somelier Association (SSA), 2018); https://londonsakechallenge.com/awarded-sake-2019/
28. *London Sake Challenge 2019: Awarded Sake* (SSA, 2019); https://londonsakechallenge.com/awarded-sake-2019/
29. Yasuhara, M., Hayashi, T. & Asai, K. Overview of the special issue "Groundwater in Mt. Fuji". *J. Geogr.* **126**, 25–27 (2017).
30. Yasuhara, M., Hayashi, T., Asai, K., Uchiyama, M. & Nakamura, T. Overview of the special issue "Groundwater in Mt. Fuji (Part 2)". *J. Geogr.* **129**, 657–660 (2020).
31. Gmati, S., Tase, N., Tsujimura, M. & Tosaki, Y. Aquifers interaction in the southwestern foot of Mt. Fuji, Japan, examined through hydrochemistry and statistical analyses. *Hydrol. Res. Lett.* **5**, 58–63 (2011).

32. Ikeda, K. Water-sediments interaction of salinized groundwater, and its chemical compositions in coastal areas (in Japanese). *Jpn. J. Limnol.* **46**, 303–314 (1985).
33. Kato, K. et al. Unveiled groundwater flushing from the deep seafloor in Suruga Bay. *Limnology* https://doi.org/10.1007/s10201-014-0445-0 (2015).
34. Segawa, T. et al. Microbes in groundwater of a volcanic mountain, Mt. Fuji; 16S rDNA phylogenetic analysis as a possible indicator for the transport routes of groundwater. *Geomicrobiol. J.* **32**, 677–688 (2015).
35. Sugiyama, A., Masuda, S., Nagaosa, K., Tsujimura, M. & Kato, K. Tracking the direct impact of rainfall on groundwater at Mt. Fuji by multiple analyses including microbial DNA. *Biogeosciences* **15**, 721–732 (2018).
36. Yasuhara, M., Kazahaya, K. & Marui, A. in *Fuji Volcano* (eds Aramaki, S. et al.) 389–405 (Yamanashi Institute of Environmental Sciences, 2007).
37. Tsuchi, R. in *Fuji Volcano* (eds Aramaki, S. et al.) 375–387 (Yamanashi Institute of Environmental Sciences, 2007).
38. Takada, A., Yamamoto, T., Ishizuka, Y. & Nakano, S. in *Miscellaneous Map Series* No. 12, 56 (Geological Survey of Japan (GSJ), National Institute of Advanced Industrial Science and Technology (AIST), 2016).
39. Uchiyama, T. Hydrogeological structure and hydrological characterization in the northern foot area of Fuji volcano, central Japan (in Japanese). *J. Geogr.* **129**, 697–724 (2020).
40. Ikawa, R. et al. in *S-5: Seamless Geoinformation of Coastal Zone "Northern Coastal Zone of Suruga Bay"* (GSJ, AIST, 2016).
41. AIST *2014 Marine Geological and Environmental Survey Confirmation Technology Development Results Report* (in Japanese) (AIST, 2015).
42. AIST *2015 Marine Geological and Environmental Survey Confirmation Technology Development Results Report* (in Japanese) (AIST, 2016).
43. Lin, A., Iida, K. & Tanaka, H. On-land active thrust faults of the Nankai–Suruga subduction zone: the Fujikawa-kako Fault Zone, central Japan. *Tectonophysics* **601**, 1–19 (2013).
44. Fujita, E. et al. Stress field change around the Mount Fuji volcano magma system caused by the Tohoku megathrust earthquake, Japan. *Bull. Volcanol.* **75**, 679 (2013).
45. Kano, K.-I., Odawara, K., Yamamoto, G. & Ito, T. Tectonics of the Fujikawa-kako Fault Zone around the Hoshiyama Hills, central Japan, since 1 Ma. *Geosci. Rep. Shizuoka Univ.* **46**, 19–49 (2019).
46. Schilling, O. S., Cook, P. G. & Brunner, P. Beyond classical observations in hydrogeology: the advantages of including exchange flux, temperature, tracer concentration, residence time and soil moisture observations in groundwater model calibration. *Rev. Geophys.* **57**, 146–182 (2019).
47. Schilling, O. S. et al. Quantifying groundwater recharge dynamics and unsaturated zone processes in snow-dominated catchments via on-site dissolved gas analysis. *Water Resour. Res.* **57**, e2020WR028479 (2021).
48. *National Hydrological Environment Database of Japan* (GSJ, AIST, 2020).
49. Hayashi, T. Understanding the groundwater flow system at the northern part of Mt. Fuji: current issues and prospects (in Japanese). *J. Geogr.* **129**, 677–695 (2020).
50. Yasuhara, M., Marui, A., & Kazahaya, K. (1997). Stable isotopic composition of groundwater from Mt. Yatsugatake and Mt. Fuji, Japan. Proceedings of the Rabat Symposium. Rabat Symposium, April 1997, Wallingford, UK.
51. Jasechko, S. Global isotope hydrogeology—review. *Rev. Geophys.* https://doi.org/10.1029/2018RG000627 (2019).
52. Yaguchi, M., Muramatsu, Y., Chiba, H., Okumura, F. & Ohba, T. The origin and hydrochemistry of deep well waters from the northern foot of Mt. Fuji, central Japan. *Geochem. J.* **50**, 227–239 (2016).
53. Aizawa, K. et al. Gas pathways and remotely triggered earthquakes beneath Mount Fuji, Japan. *Geology* **44**, 127–130 (2016).
54. Kipfer, R. et al. Injection of mantle type helium into Lake Van (Turkey): the clue for quantifying deep water renewal. *Earth Planet. Sci. Lett.* **125**, 357–370 (1994).
55. Kipfer, R., Aeschbach-Hertig, W., Peeters, F. & Stute, M. in *Noble Gases in Geochemistry and Cosmochemistry* Reviews in Mineralogy and Geochemistry Vol. 47 (eds Porcelli, D. et al.) Ch. 14 (De Gruyter, 2002).
56. Sano, Y. & Fischer, T. P. in *The Noble Gases as Geochemical Tracers: Advances in isotope geochemistry* (ed. Burnard, O.) Ch. 10 (Springer, 2013).
57. Sano, Y. & Wakita, H. Distribution of $^{3}He/^{4}He$ ratios and its implications for geotectonic structure of the Japanese Islands. *J. Geophys. Res.* **90**, 8729–8741 (1985).
58. Tomonaga, Y. et al. Fluid dynamics along the Nankai Trough: He isotopes reveal direct seafloor mantle-fluid emission in the Kumano Basin (Southwest Japan). *ACS Earth Space Chem.* **4**, 2015–2112 (2020).
59. Chen, A. et al. Mantle fluids associated with crustal-scale faulting in a continental subduction setting, Taiwan. *Sci Rep.* **9**, 10805 (2019).
60. Crossey, L. J. et al. Continental smokers couple mantle degassing and distinctive microbiology within continents. *Earth Planet. Sci. Lett.* **435**, 22–30 (2016).
61. Crossey, L. J. et al. Degassing of mantle-derived CO_2 and He from springs in the southern Colorado Plateau region—neotectonic connections and implications for groundwater systems. *Geol. Soc. Am. Bull.* **121**, 1034–1053 (2009).
62. Kusuda, C., Iwamori, H., Nakamura, H., Kazahaya, K. & Morikawa, N. Arima hot spring waters as a deep-seated brine from subducting slab. *Earth Planets Space* **66**, 119 (2014).
63. Sano, Y., Kameda, A., Takahata, N., Yamamoto, J. & Nakajima, J. Tracing extinct spreading center in SW Japan by helium-3 emanation. *Chem. Geol.* **266**, 50–56 (2009).
64. Sano, Y. et al. Groundwater helium anomaly reflects strain change during the 2016 Kumamoto earthquake in Southwest Japan. *Sci. Rep.* **6**, 37939 (2016).
65. Peeters, F. et al. Improving noble gas based paleoclimate reconstruction and groundwater dating using $^{20}Ne/^{22}Ne$ ratios. *Geochim. Cosmochim. Acta* **67**, 587–600 (2002).
66. Reimann, C. & de Caritat, P. *Chemical Elements in the Environment* 398 (Springer, 1998).
67. Hamada, T. in *Vanadium in the Environment. Part 1: Chemistry and Biochemistry* Advances in Environmental Sciences and Technology Vol. 10 (ed. Nriagu, J. O.) 97–123 (Wiley & Sons, 1998).
68. Koshimizu, S. & Kyotani, T. Geochemical behaviors of multi-elements in water samples from the Fuji and Sagami Rivers, Central Japan, using vanadium as an effective indicator. *Jpn J. Limnol.* **63**, 113–124 (2002).
69. Sohrin, R. in *Green Science and Technology* (eds Park, E. Y. et al.) Ch. 7 (CRC, 2019).
70. Wehrli, B. & Stumm, W. Oxygenation of vanadyl(IV). Effect of coordinated surface hydroxyl groups and hydroxide ion. *Langmuir* **4**, 753–758 (1988).
71. Wright, M. T. & Belitz, K. Factors controlling the regional distribution of vanadium in groundwater. *Ground Water* **48**, 515–525 (2010).
72. Deverel, S. J., Goldberg, S. & Fujii, R. in *Agricultural salinity assessment and management* (eds W.W. Wallender & K.K. Tanji) 89–137 (American Society of Civil Engineers, 2012).
73. Wehrli, B. & Stumm, W. Vanadyl in natural waters: adsorption and hydrolysis promote oxygenation. *Geochim. Cosmochim. Acta* **53**, 69–77 (1989).

74. Chen, G. & Liu, H. Understanding the reduction kinetics of aqueous vanadium(V) and transformation products using rotating ring-disk electrodes. *Environ. Sci. Technol.* **51**, 11643–11651 (2017).
75. Telfeyan, K., Johannesson, K. H., Mohajerin, T. J. & Palmore, C. D. Vanadium geochemistry along groundwater flow paths in contrasting aquifers of the United States: Carrizo Sand (Texas) and Oasis Valley (Nevada) aquifers. *Chem. Geol.* **410**, 63–78 (2015).
76. Kan, K. et al. Archaea in Yellowstone Lake. *ISME J.* **5**, 1784–1795 (2011).
77. Wong, H. L. et al. Dynamics of archaea at fine spatial scales in Shark Bay mat microbiomes. *Sci. Rep.* **7**, 46160 (2017).
78. Ikeda, K. A study on chemical characteristics of ground water in Fuji area (in Japanese). *J. Groundw. Hydrol.* **24**, 77–93 (1982).
79. Aizawa, K. et al. Hydrothermal system beneath Mt. Fuji volcano inferred from magnetotellurics and electric self-potential. *Earth Planet. Sci. Lett.* **235**, 343–355 (2005).
80. Yamamoto, T., Takada, A., Ishizuka, Y., Miyaji, N. & Tajima, Y. Basaltic pyroclastic flows of Fuji volcano, Japan: characteristics of the deposits and their origin. *Bull. Volcanol.* **67**, 622–633 (2005).
81. Yamamoto, T., Takada, A., Ishizuka, Y. & Nakano, S. Chronology of the products of Fuji volcano based on new radiometoric carbon ages (in Japanese). *Bull. Volcanol.* **50**, 53–70 (2005).
82. Aizawa, K., Yoshimura, R. & Oshiman, N. Splitting of the Philippine Sea Plate and a magma chamber beneath Mt. Fuji. *Geophys. Res. Lett.* **31**, L09603 (2004).
83. Nakamura, H., Iwamori, H. & Kimura, J.-I. Geochemical evidence for enhanced fluid flux due to overlapping subducting plates. *Nat. Geosci.* **1**, 380–384 (2008).
84. Kaneko, T., Yasuda, A., Fujii, T. & Yoshimoto, M. Crypto-magma chambers beneath Mt. Fuji. *J. Volcanol. Geotherm. Res.* **193**, 161–170 (2010).
85. Tsuya, H., Machida, H., & Shimozuru, D. (1988). Geology of volcano Mt. Fuji. Explanatory text of the geologic map of Mt. Fuji (scale 1:50,000; second printing). Geological Survey of Japan (GSJ), Tsukuba, Japan.
86. Yoshimoto, M. et al. Evolution of Mount Fuji, Japan: inference from drilling into the subaerial oldest volcano, pre-Komitake. *Isl. Arc.* **19**, 470–488 (2010).
87. Shikazono, N., Arakawa, T. & Nakano, T. Groundwater quality, flow, and nitrogen pollution at the southern foot of Mt. Fuji (in Japanese). *J. Geogr.* **123**, 323–342 (2014).
88. Tosaki, Y., Tase, N., Sasa, K., Takahashi, T. & Nagashima, Y. Estimation of groundwater residence time using the 36Cl bomb pulse. *Groundwater* **49**, 891–902 (2011).
89. Yamamoto, T. *Geology of the Southwestern Part of Fuji Volcano* (in Japanese) 27 (GSJ, AIST, 2014).
90. Tsuya, H. *Geology of volcano Mt. Fuji. Explanatory text of the geologic map of Mt. Fuji (scale 1:50,000)*. Geological Survey of Japan, Tsukuba, Japan. (1968).
91. Tomiyama, S., Ii, H., Miyaike, S., Hattori, R. & Ito, Y. Estimation of the sources and flow system of groundwater in Fuji-Gotenba area by stable isotopic analysis and groundwater flow simulation (in Japanese). *Bunseki Kagaku* **58**, 865–872 (2009).
92. Oguchi, T. & Oguchi, C. T. in *Geomorphological Landscapes of the World* (ed. Migoń, P.) Ch. 31 (Springer, 2010).
93. *Mean Annual Precipitation from 1981-2010 Recorded at the Four Mt. Fuji Observatories (Mishima, Fuji, Furuseki, Yamanaka)* (Japan Meteorological Agency, 2015).
94. Schilling, O. S., Park, Y.-J., Therrien, R. & Nagare, R. M. Integrated surface and subsurface hydrological modeling with snowmelt and pore water freeze-thaw. *Groundwater* **57**, 63–74 (2018).
95. Sakio, H. & Masuzawa, T. Advancing timberline on Mt. Fuji between 1978 and 2018. *Plants* **9**, 1537 (2020).
96. Asai, K. & Koshimizu, S. $^{3}H/^{3}He$-based groundwater ages for springs located at the foot of Mt. Fuji (in Japanese). *J. Groundw. Hydrol.* **61**, 291–298 (2019).
97. Sakai, Y., Shita, K., Koshimizu, S. & Tomura, K. Geochemical study of trace vanadium in water by preconcentrational neutron activation analysis. *J. Radioanal. Nucl. Chem.* **216**, 203–212 (1997).
98. Nahar, S. & Zhang, J. Concentration and distribution of organic and inorganic water pollutants in eastern Shizuoka, Japan. *Toxicol. Environ. Chem*. https://doi.org/10.1080/02772248.2011.610498 (2011).
99. Kamitani, T., Watanabe, M., Muranaka, Y., Shin, K.-C. & Nakano, T. Geographical characteristics and sources of dissolved ions in groundwater at the southern part of Mt. Fuji (in Japanese). *J. Geogr.* **126**, 43–71 (2017).
100. Kawagucci, S. et al. Disturbance of deep-sea environments induced by the M9.0 Tohoku earthquake. *Sci Rep.* **2**, 270 (2012).
101. Uchida, N. & Bürgmann, R. A decade of lessons learned from the 2011 Tohoku-Oki earthquake. *Rev. Geophys.* **59**, e2020RG000713 (2021).
102. Mahara, Y., Igarashi, T. & Tanaka, Y. Groundwater ages of confined aquifer in Mishima lava flow, Shizuoka (in Japanese). *J. Groundw. Hydrol.* **35**, 201–215 (1993).
103. Nakamura, T. et al. Sources of water and nitrate in springs at the northern foot of Mt. Fuji and nitrate loading in the Katsuragawa River (in Japanese). *J. Geogr.* **126**, 73–88 (2017).
104. Notsu, K., Mori, T., Sumino, H. & Ohno, M. in *Fuji Volcano* (eds Aramaki, S. et al.) 173–182 (Yamanashi Institute of Environmental Sciences, 2007).
105. Ogata, M. & Kobayashi, H. *Hydrologic Science Research for the Management and Utilization of Ground Water Resources in the Northern Piedmont Area of Mt. Fuji: Fluorine Ion and Vanadium Contained in Ground Water at the Northern Foot of Mt. Fuji* (Yamanashi Industrial Technology Center, 2015).
106. Ogata, M., Kobayashi, H. & Koshimizu, S. Concentration of fluorine in groundwater and groundwater table at the northern foot of Mt. Fuji (in Japanese). *J. Groundw. Hydrol.* **56**, 35–51 (2014).
107. Ohno, M., Sumino, H., Hernandez, P. A., Sato, T. & Nagao, K. Helium isotopes in the Izu Peninsula, Japan: relation of magma and crustal activity. *J. Volcanol. Geotherm. Res.* **199**, 118–126 (2011).
108. Okabe, S., Shibasaki, M., Oikawa, T., Kawaguchi, Y. & Nihongi, H. Geochemical studies of spring and lake waters on and around Mt. Fuji (in Japanese). *J. Sch. Mar. Sci. Technol. Tokai Univ.* **14**, 81–105 (1981).
109. Ono, M., Ikawa, R., Machida, H. & Marui, A. Distribution of radon concentration in groundwater at the southwestern foot of Mt. Fuji (in Japanese). *Radioisotopes* **65**, 431–439 (2016).
110. Tosaki, Y. *Estimation of Groundwater Residence Time Using Bomb-Produced Chlorine-36*. PhD thesis, Univ. Tsukuba (2008).
111. Umeda, K., Asamori, K. & Kusano, T. Release of mantle and crustal helium from a fault following an inland earthquake. *Appl. Geochem.* **37**, 134–141 (2013).
112. Yamamoto, C. *Estimation of Groundwater Flow System Using Multi-tracer Techniques in Mt. Fuji, Japan*. (in Japanese) PhD thesis, Univ. Tsukuba (2016).
113. Yamamoto, S. & Nakamura, T. Visit to valuable water springs (129) valuable water at the northern foot of Mount Fuji (Fuji-Kawaguchiko Town) (in Japanese). *J. Groundw. Hydrol.* **62**, 329–336 (2020).
114. Yamamoto, S. et al. Water sources of lake bottom springs in Lake Kawaguchi, northern foot of Mount Fuji, Japan (in Japanese). *J. Geogr.* **129**, 665–676 (2020).
115. Yamamoto, S., Nakamura, T. & Uchiyama, T. Newly discovered lake bottom springs from Lake Kawaguchi, the northern foot of Mount Fuji, Japan (in Japanese). *J. Jpn Assoc. Hydrol. Sci.* **47**, 49–59 (2017).

116. Yamamoto, S., Nakamura, T., Koishikawa, H. & Uchiyama, T. Water quality of shallow groundwater in the southern coast area of Lake Kawaguchi at the northern foot of Mt. Fuji, Yamanashi, Japan (in Japanese). *Mt Fuji Res.* **11**, 1–9 (2017).
117. Coplen, T. B. Reporting of stable hydrogen, carbon, and oxygen isotopic abundances. *Geothermics* **66**, 273–276 (1994).
118. Nimz, G. J. in *Isotope Tracers in Catchment Hydrology* (eds Kendall, C. & McDonnell, J. J.) Ch. 8 (Elsevier, 1998).
119. Bullen, T. D. & Kendall, C. in *Isotope Tracers in Catchment Hydrology* (eds Kendall, C. & McDonnell, J. J.) Ch. 18 (Elsevier, 1998).
120. *Vanadium Pentoxide and Other Inorganic Vanadium Compounds* Vol. 29 (WHO, 2001).
121. Nagai, T., Takahashi, M., Hirahara, Y. & Shuto, K. Sr-Nd isotopic compositions of volcanic rocks from Fuji, Komitake and Ashitaka Volcanoes, Central Japan (in Japanese). *Proc. Inst. Nat. Sci. Nihon Univ.* **39**, 205–215 (2004).
122. Hogan, J. F. & Blum, J. D. Tracing hydrologic flow paths in a small forested watershed using variations in $^{87}Sr/^{86}Sr$, [Ca]/[Sr], [Ba]/[Sr] and $\delta^{18}O$. *Water Resour. Res.* **39**, 1282 (2003).
123. Koshikawa, M. K. et al. Using isotopes to determine the contribution of volcanic ash to Sr and Ca in stream waters and plants in a granite watershed, Mt. Tsukuba, central Japan. *Environ. Earth Sci.* **75**, 501 (2016).
124. Graustein, W. C. in *Stable Isotopes in Ecological Research Ecological Studies (Analysis and Synthesis)* (eds Rundel, JP.W. et al.) Ch. 28 (Springer, 1989).
125. Cook, P. G. & Böhlke, J.-K. in *Environmental Tracers in Subsurface Hydrology* (eds Cook, P. G. & Herczeg, A. L.) Ch. 1 (Springer, 2000).
126. Aeschbach-Hertig, W. & Solomon, D. K. in *The Noble Gases as Geochemical Tracers* (ed. Burnard, P.) Ch. 5 (Springer, 2013).
127. Popp, A. L. et al. A framework for untangling transient groundwater mixing and travel times. *Water Resour. Res.* **57**, e2020WR028362 (2021).
128. Schilling, O. S. et al. Advancing physically-based flow simulations of alluvial systems through observations of ^{222}Rn, $^{3}H/^{3}He$, atmospheric noble gases and the novel ^{37}Ar tracer method. *Water Resour. Res.* **53**, 10465–10490 (2017).
129. Tomonaga, Y. et al. Using noble-gas and stable-isotope data to determine groundwater origin and flow regimes: applicatoin to the Ceneri Base Tunnel (Switzerland). *J. Hydrol.* **545**, 395–409 (2017).
130. Niu, Y. et al. Noble gas signatures in the island of Maui, Hawaii – characterizing groundwater sources in fractured systems. *Water Resour. Res.* **53**, 3599–3614 (2017).
131. Warrier, R. B., Castro, M. C. & Hall, C. M. Recharge and source-water insights from the Galapagos Islands using noble gases and stable isotopes. *Water Resour. Res.* https://doi.org/10.1029/2011WR010954 (2012).
132. Schilling, O. S. et al. Buried paleo-channel detection with a groundwater model, tracer-based observations, and spatially varying, preferred anisotropy pilot point calibration. *Geophys. Res. Lett.* **49**, e2022GL098944 (2022).
133. Brennwald, M. S., Schmidt, M., Oser, J. & Kipfer, R. A portable and autonomous mass spectrometric system for on-site environmental gas analysis. *Environ. Sci. Technol.* **50**, 13455–12463 (2016).
134. Tomonaga, Y. et al. On-line monitoring of the gas composition in the full-scale emplacement experiment at Mont Terri (Switzerland). *Appl. Geochem.* **100**, 234–243 (2019).
135. Brennwald, M. S., Tomonaga, Y. & Kipfer, R. Deconvolution and compensation of mass spectrometric overlap interferences with the miniRUEDI portable mass spectrometer. *MethodsX* **7**, 101038 (2020).
136. Van Rossum, G. & Drake, F. L. *Python 3 Reference Manual* (CreateSpace, 2009).
137. Beyerle, U. et al. A mass spectrometric system for the analysis of noble gases and tritium from water samples. *Environ. Sci. Technol.* **34**, 2042–2050 (2000).
138. Clarke, W. B., Jenkins, W. J. & Top, Z. Determination of tritium by mass spectrometric measurement of ^{3}He. *Int. J. Appl. Radiat. Isotopes* **27**, 515–522 (1976).
139. Bucci, A., Petrella, E., Celivo, F. & Naclerio, G. Use of molecular approaches in hydrogeological studies: the case of carbonate aquifers in southern Italy. *Hydrogeol. J.* **25**, 1017–1031 (2017).
140. Proctor, C. R. et al. Phylogenetic clustering of small low nucleic acid-content bacteria across diverse freshwater ecosystems. *ISME J.* **12**, 1344–1359 (2018).
141. Pronk, M., Goldscheider, N. & Zopfi, J. Microbial communities in karst groundwater and their potential use for biomonitoring. *Hydrogeol. J.* **17**, 37–48 (2009).
142. Miller, J. B., Frisbee, M. D., Hamilton, T. L. & Murugapiran, S. K. Recharge from glacial meltwater is critical for alpine springs and their microbiomes. *Environ. Res. Lett.* **16**, 064012 (2021).
143. Ginn, T. R. et al. in *Encyclopedia of Hydrological Sciences* (ed. Anderson, M.G.) Ch. 105 (John Wiley & Sons, 2005).
144. Tufenkji, N. & Emelko, M. B. in *Encyclopedia of Environmental Health* (ed. Nriagu, J.O.) Vol. 2, 715–726 (Elsevier, 2011).
145. Nevecherya, I. K., Shestakov, V. M., Mazaev, V. T. & Shlepnina, T. G. Survival rate of pathogenic bacteria and viruses in groundwater. *Water Res.* **32**, 209–214 (2005).
146. Franzosa, E. A. et al. Sequencing and beyond: integrating molecular 'omics' for microbial community profiling. *Nature Rev. Microbiol.* **13**, 360–372 (2015).
147. Kimura, H., Ishibashi, J. I., Masuda, H., Kato, K. & Hanada, S. Selective phylogenetic analysis targeting 16S rRNA genes of hyperthermophilic archaea in the deep-subsurface hot biosphere. *Appl. Environ. Microbiol.* **73**, 2110–2117 (2007).
148. Somerville, C. C., Knight, I. T., Straube, W. L. & Colwell, R. R. Simple, rapid method for direct isolation of nucleic-acids from aquatic environments. *Appl. Environ. Microbiol.* **55**, 548–554 (1989).
149. Takahashi, S., Tomita, J., Nishioka, K., Hisada, T. & Nishijima, M. Development of a prokaryotic universal primer for simultaneous analysis of bacteria and archaea using next-generation sequencing. *PLoS ONE* https://doi.org/10.1371/journal.pone.0105592 (2014).
150. Wasimuddin et al. Evaluation of primer pairs for microbiome profiling from soils to humans within the One Health framework. *Mol. Ecol. Resour.* **20**, 1558–1571 (2020).
151. Suzuki, Y., Shimizu, H., Kuroda, T., Takada, Y. & Nukazawa, K. Plant debris are hotbeds for pathogenic bacteria on recreational sandy beaches. *Sci Rep.* **11**, 11496 (2021).
152. Bolyen, E. et al. Reproducible, interactive, scalable and extensible microbiome data science using QIIME 2. *Nat. Biotechnol.* **37**, 852–857 (2019).
153. Caporaso, J. G. et al. QIIME allows analysis of high- throughput community sequencing data. *Nat. Methods* **7**, 335–336 (2010).
154. McDonald, D. et al. An improved Greengenes taxonomy with explicit ranks for ecological and evolutionary analyses of bacteria and archaea. *ISME J.* **6**, 610–618 (2012).
155. DeSantis, T. Z. et al. Greengenes, a chimera-checked 16S rRNA gene database and workbench compatible with ARB. *Appl. Environ. Microbiol.* **72**, 5069–5072 (2006).
156. McMurdie, P. J. & Holmes, S. phyloseq: an R package for reproducible interactive analysis and graphics of microbiome census data. *PLoS ONE* **8**, e61217 (2013).
157. R: A Language and Environment for Statistical Computing v.3.6.2 (R Foundation for Statistical Computing, 2019).

158. Porter, K. G. & Feig, Y. S. The use of DAPI for identifying and counting aquatic microflora. *Limnol. Oceanogr.* **25**, 943–948 (1980).
159. Schilling, O. S. et al. Mt. Fuji hydrogeochemical and microbiological dataset. *HydroShare* https://doi.org/10.4211/hs.4eac370d12e142b5aa718e5deb57da39 (2022).
160. Gotelli, N. J. & Chao, A. in *Encyclopedia of Biodiversity* Vol. 5 (ed. Levin, S. A.) 195–211 (Academic, 2013).
161. *World Imagery* (Esri, 2021); https://www.arcgis.com/home/item.html?id=10df2279f9684e4a9f6a7f08febac2a9
162. *Elevation Tile Map of Japan (DEM5A; Resolution: 5m)* (Geospatial Information Authority of Japan (GSI), 2021).
163. Chiba, T., Kaneta, S. & Suzuki, Y. in *The International Archives of the Photogrammetry* Vol. XXXVII Ch. B2 (Remote Sensing and Spatial Information Sciences, 2008).
164. Air Asia Survey Co. Ltd *Red Relief Image Map of Japan (RRIM 10_2016)* (GSI, 2016).
165. *Active Fault Database of Japan April 26 2019 edn* Disclosure database DB095 (AIST, 2019).
166. Bird, P. An updated digital model of plate boundaries. *Geochem. Geophys. Geosyst.* https://doi.org/10.1029/2001GC000252 (2003).
167. Van Horne, A., Sato, H. & Ishiyama, T. Evolution of the Sea of Japan back-arc and some unsolved issues. *Tectonophysics* **710–711**, 6–20 (2017).
168. Shannon, C. E. A mathematical theory of communication. *Bell Syst. Tech. J.* **27**, 379–423 (1948).
169. *2019 Coastal Disposal System Evaluation Confirmation Technology Results Report* (in Japanese) (AIST, 2019).

Acknowledgements

We thank A. Lightfoot, S. Giroud, K. Mori, N. Murai, M. Tsujimura and U. Tsunogai for technical assistance. O.S.S. gratefully acknowledges funding provided by the Swiss National Science Foundation (SNSF) via grant number P2NEP2_171985 during part of this study, and P.B. acknowledges funding received via SNSF project grant number 200021_179017. This study was also supported by the River Works Technology Research and Development Program from the Ministry of Land, Infrastructure, Transport and Tourism, Japan.

Author contributions

O.S.S., K.K., P.B. and R.K. conceived the study. O.S.S., K.N., K.K., T.U.S., Y.T. and M.S.B. designed and performed the field sampling experiments. O.S.S., N.K., R.S., Y.T. and M.S.B. conducted the laboratory-based analyses. O.S.S. collected literature data, prepared the databases, processed and analysed the data, prepared figures and tables, and wrote the manuscript. O.S.S., R.K., Y.T., M.S.B., P.B. and K.K. edited the manuscript.

Competing interests

The authors declare no competing interests.

Additional information

Supplementary information The online version contains supplementary material available at https://doi.org/10.1038/s44221-022-00001-4.

Correspondence and requests for materials should be addressed to O. S. Schilling.

Peer review information *Nature Water* thanks Daniele Pinti and the other, anonymous, reviewer(s) for their contribution to the peer review of this work.